# Unmodified Homogeneous Rhodium-Catalyzed Hydroformylation of Styrene. The Detailed Kinetics of the Regioselective Synthesis

Jinhai Feng and Marc Garland*

*Department of Chemical Engineering, 10 Kent Ridge Crescent, National University of Singapore, Singapore 119260*

*Received June 22, 1998*

The homogeneous regioselective catalytic hydroformylation of styrene to (±)-2-phenylpropanal and 3-phenylpropanal was studied starting with $Rh_4(CO)_{12}$ as catalyst precursor in *n*-hexane as solvent. The reaction conditions were $T = 298-313$ K, $P_{H2} = 0.27-1.01$ MPa (0.002−0.0074 mol fraction), $P_{CO} = 3.0-6.0$ MPa (0.042−0.075 mol fraction), $[Rh_4(CO)_{12}]_o = 3.5 \times 10^{-5}$ to $1.7 \times 10^{-4}$ mol fraction, and $[C_8H_8]_o = 0.118-0.349$ mol fraction. Quantitative high-pressure in-situ infrared spectroscopic measurements were made under isobaric and isothermal conditions during the 5-h kinetic experiments. In all experiments, the disappearance of the precursor $Rh_4(CO)_{12}$ resulted in the formation of two observable acyl intermediates, namely the major isomer (±)-$PhCH(CH_3)CORh(CO)_4$ and the minor isomer $PhCH_2CH_2CORh(CO)_4$. Clean, high-signal-to-noise spectra of the two intermediates (±)-$PhCH(CH_3)CORh(CO)_4$ and $PhCH_2CH_2CORh(CO)_4$ were obtained. The disappearance of $Rh_4(CO)_{12}$ was found to followed the rate expression rate $= k_o^{\alpha}[Rh_4(CO)_{12}]^{1.0}[CO]^{1.3}[H_2]^{0.9}[C_8H_8]^{0.15}$ where $k_o^{\alpha} = (\kappa T/h)\exp(-62.6\ \text{kJ/(mol}\ RT)) + 37.2\ \text{J/(mol}\ R))$. This rate expression suggests that cluster fragmentation of $Rh_4(CO)_{12}$ proceeds via CO addition and polyhedron opening as the first step. The hydrogenolysis of (±)-$PhCH(CH_3)CORh(CO)_4$ to yield the major product (±)-$PhCH(CH_3)CHO$ was found to follow the rate expression rate $= k_o^{\beta}[PhCH(CH_3)CORh(CO)_4]^{1.0}[CO]^{-1.0}[H_2]^{1.0}[C_8H_8]^{0.0}$ with $k_o^{\beta} = (\kappa T/h)\exp(-78.8\ \text{kJ/(mole RT)} + 15.2\ \text{J/(mol}\ R)$, and the hydrogenolysis of $PhCH_2CH_2CORh(CO)_4$ to yield the minor product $PhCH_2CH_2CHO$ was found to follow the rate expression rate $= k_o^{\gamma}[PhCH_2CH_2CORh(CO)_4]^{1.0}[CO]^{-1.0}[H_2]^{1.0}[C_8H_8]^{0.0}$ with $k_o^{\gamma} = (\kappa T/h)\exp(-113\ \text{kJ/(mol}\ RT)) - 102\ \text{J/(mol}\ R)$. The two rate expressions for hydrogenolysis are consistent with (1) equilibrium controlled dissociation of a CO ligand from the acyl intermediates to form coordinatively unsaturated species, (2) a rate-limiting step involving hydrogen activation on the 4-coordinate species, and (3) product formation accompanied by the formation of a transient species $\{HRh(CO)_3\}$.



## Introduction

Since the first patents concerning the application of rhodium, particularly in the forms $Rh_4(CO)_{12}$ and $Rh_6(CO)_{16}$,[1] the unmodified homogeneous rhodium-catalyzed hydroformylation reaction has been the subject of numerous mechanistic studies.[2,3] For example, early kinetic studies with α and internal alkenes have indicated that the reaction orders are normally 1.0 with the respect to rhodium,[4] 1.0 with respect to hydrogen, and −1.0 with respect to carbon monoxide.[5] Furthermore, direct spectroscopic evidence for cluster fragmentation, under syngas, particularly to $Rh_2(CO)_8$ and $HRh(CO)_4$ had been obtained,[6] and strong indirect experimental evidence for the existence of mononuclear acyl rhodium tetracarbonyls in the catalysis had been gathered.[7] Consequently, a widely accepted mechanism for a single product hydroformylation has developed and is shown in Scheme 1.[3]

In the past 10 years, extensive in-situ spectroscopic studies have been performed on the hydroformylation of 3,3-dimethylbut-1-ene and cyclohexene.[8−11] In these studies, the fragmentation of $Rh_4(CO)_{12}$ and the formation of mononuclear acyl rhodium tetracarbonyls $RCORh(CO)_4$ (R = $-CH_2CH_2C(CH)_3$, $-C_6H_{11}$) as the only obervable intermediates under reaction conditions has been repeatedly shown.[12] In addition, the detailed kinetics of the fragmentation reaction (eq 1) and the kinetics of the hydrogenolysis of the acyl rhodium intermediates

(1) (a) Schiler, G. (Che. Verwertungsges. Oberhausen), Ger Pat. 965,-605, 1956; *Chem Abst.* **1959**, *53*, 11226. (b) Hughes, V. L. (Esso Res Eng Co.) U.S. Pat. 2.880.241, 1959; *Chem. Abst.* **1959**, *53*, 14938. (c) Hughes, V. L. (Esso Res. Eng. Co.) Br. Pat. 801.734, 1958; *Chem Abst.* **1959**, *53*, 7014.

(2) Marko, L. In *Aspects of Homogeneous Catalysis*; Ugo, R., Ed, Reidel: Dordrecht, The Netherlands, 1974; Vol. II.

(3) Dickson, R. S. *Homogeneous Catalysis with Compounds of Rhodium and Iridum*; Reidel: Dordrecht, The Netherlands, 1986.

(4) Csontos, G.; Heil, B.; Marko, L. *Ann. N.Y. Acad. Sci.* **1974**, *239*, 47.

(5) Heil, B.; Marko, L. *Chem. Ber.* **1968**, *101*, 2209.

(6) (a) Whyman, R. J. *Chem Soc. Dalton Trans.* **1972**, 1375. (b) Oldani, F.; Bor, G. *J. Organomet. Chem.* **1983**, *246*, 309. (c) Vidal J. L.; Walker, W. E. *Inorg. Chem.* **1981**, *20*, 249.

(7) Heil, B.; Marko, L.; Bor, G. *Chem Ber.* **1971**, *104*, 3418.

(8) Garland, M.; Bor, G. *Inorg. Chem.* **1989**, *28*, 410.

(9) Garland, M.; Pino, P. *Organometallics* **1991**, *10*, 1693.

(10) Garland, M. *Organometallics* **1993**, *12*, 535.

(11) Fyhr, Ch.; Garland, M. *Organometallics* **1993**, *12*, 1753.

(12) Other precursors such as $Rh_6(CO)_{16}$, $Rh_2(CO)_4Cl_2$, $CoRh(CO)_7$, and $CoRh(CO)_{12}$ have also been used.[10]

10.1021/om980514v CCC: $18.00 
Publication on Web 01/08/1999

**Scheme 1. Classic Unicyclic Catalytic Mechanism for the Unmodified Rhodium-Catalyzed Hydroformylation Reaction**

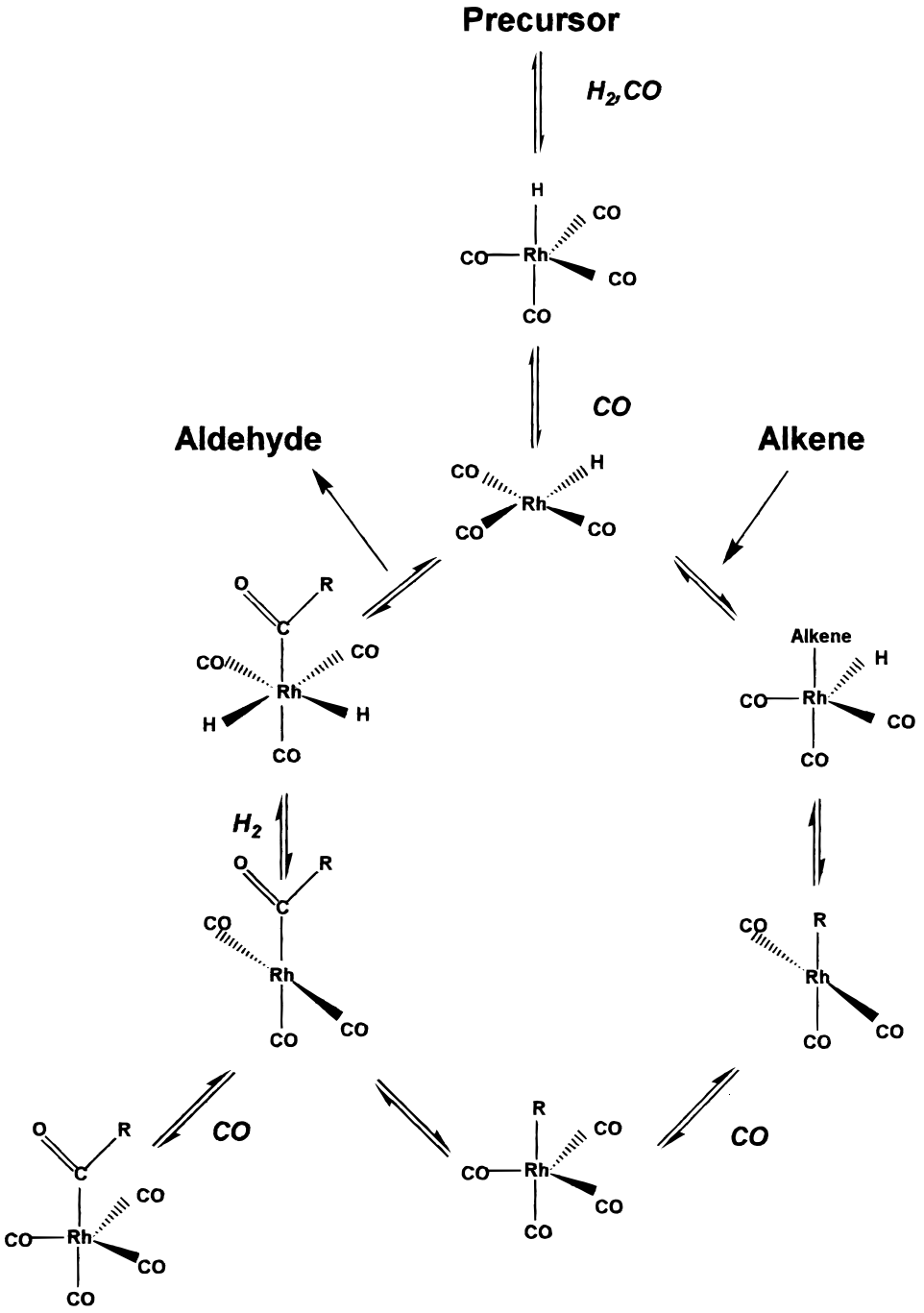




have been experimentally determined (eq 2). Over 20 different acyl rhodium tetracarbonyls have been observed under reaction conditions and characterized.[13]

$$Rh_4(CO)_{12} + 8CO + 2H_2 + 4\text{alkene} \rightarrow 4RCORh(CO)_4 \quad (1)$$

$$RCORh(CO)_4 + H_2 \rightarrow RCHO + HRh(CO)_3 + CO \quad (2)$$

Thus far, the objective of the the above-mentioned in-situ studies has been the understanding of the kinetics of single-product hydroformylations. Single-product hydroformylations, such as those arizing from the sterically hindered α alkene 3,3-dimethylbut-1-ene as well as the internal alkene cyclohexene, imply that one and only one cyclic reaction mechanism is operative. The next logical step in the understanding of unmodified rhodium-catalyzed hydroformylztion reaction would be the detailed kinetics of a regioselective synthesis. In such syntheses, two regioisomers would be formed, and their formation would arise from a single coupled dual-cycle catalytic mechanism, where each cycle contains one distinct predominant intermediate, namely an acyl rhodium tetracarbonyl.

The regioselectivity of the hydroformylation reaction has been investigated with numerous substrates. However, the use of phenyl-substituted alkenes, and par-

(13) Volker, R.; Garland, M. Manuscript in preparation.

**Scheme 2. Condensed Dual-Cycle Catalytic Mechanism for the Unmodified Rhodium-Catalyzed Hydroformylation of Styrene To Give (±)-2-Phenylpropanal and 3-Phenylpropanal**

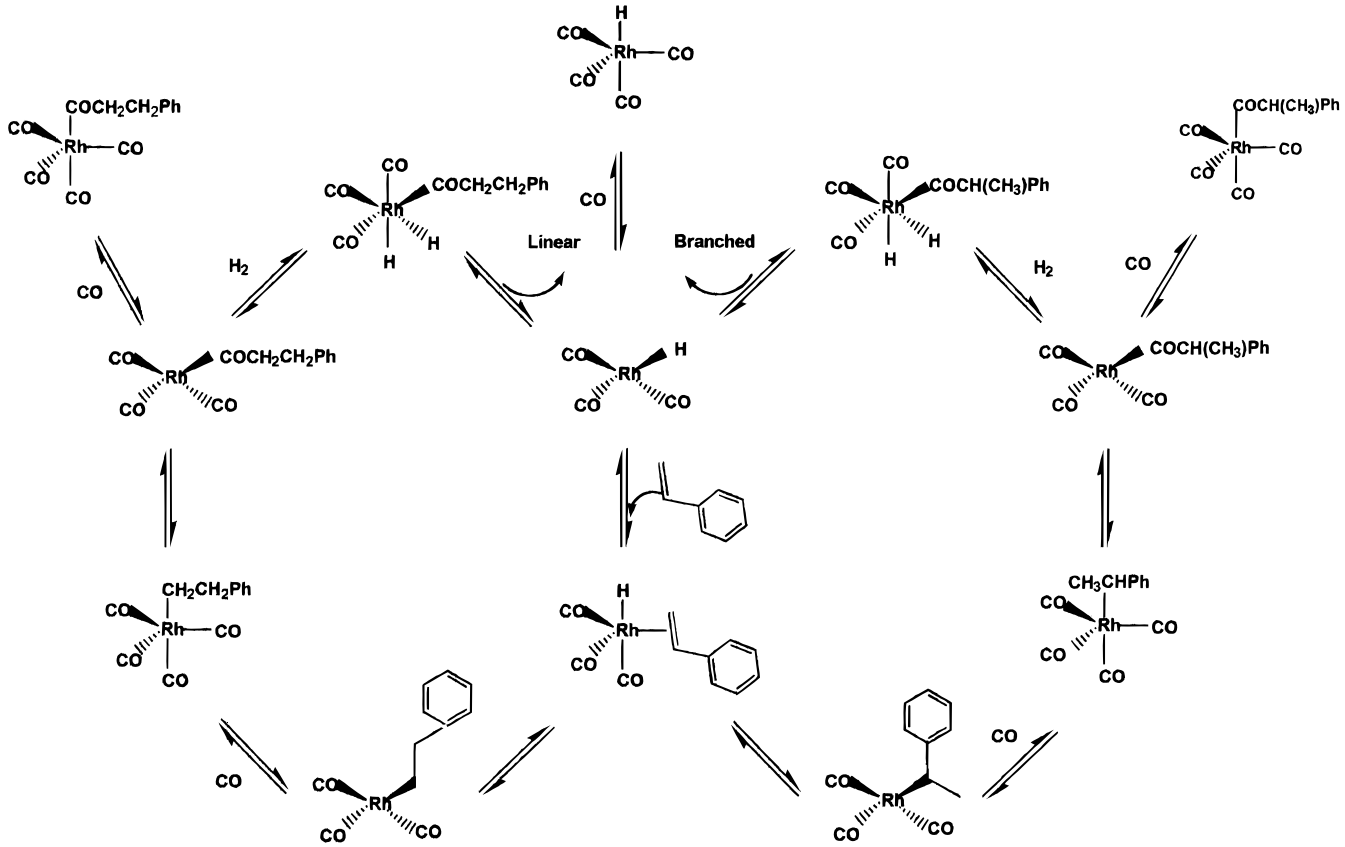




ticularly styrene,[14−16] has generated the most interest. In the unmodified rhodium-catalyzed hydroformylation of styrene, the racemic branched aldehyde is the predominent product under most reaction conditions.

$$C_6H_5CHCH_2 + CO + H_2 \rightarrow (\pm)\text{-}C_6H_5CH(CH_3)CHO \quad (3)$$

$$C_6H_5CHCH_2 + CO + H_2 \rightarrow C_6H_5CH_2CH_2CHO \quad (4)$$

In the following, an in-situ spectrocopic study of the unmodified rhodium-catalyzed hydroformylation of styrene is reported. In addition, the detailed kinetics of the regioselective syntheses of (±)-$PhCH(CH_3)CHO$ and $PhCH_2CH_2CHO$ are examined. Extending the classic mechanism for a single-product synthesis to a regioselective synthesis yields the dual-cycle mechanism shown in Scheme 2, where it is implicit that the racemic part is condensed into one cycle.

## Experimental Section

**General Information.** All solution preparations and transfers were carried out under nitrogen (99.95% Saxol, Singapore) or argon (99.95% Saxol, Singapore) atmosphere using standard Schlenk techniques.[17] Both gases were passes through deoxy and zeolite columns before use. $Rh_4(CO)_{12}$ was purchased from Strem Chemicals (Newport, MA) and was used as obtained. Puriss quality *n*-hexane (Fluka AG, Buchs, Switzerland) was refluxed from sodium potassium alloy under argon. Puriss quality (±)-2-phenylpropanal and 3-phenylpropanal (99%, Merck, Darmstadt, Germany) were used as obtained for calibrations. Reactions were carried out under carbon monoxide (99.97% British Oxygen Company) and hydrogen (99.999% Saxol, Singapore) after further purification through deoxy and zeolite columns.

The puriss quality styrene obtained for this study (Fluka AG) contained 2% ethylbenzene as impurity, as determined by GC analysis using a 10-m capillary column; HP Series 5, 30 $\mu$m-fused silica column (HP, Singapore). The styrene was distilled from $CaH_2$ and stored under argon at 273 K.

**Equipment.** Kinetic studies were performed in a 1.5-L stainless steel (SS316) autoclave (Büchi-Uster, Switzerland) which was connected to a high-pressure infrared cell. The autoclave ($P_{max}$ = 22.5 MPa) was equipped with a packed magnetic stirrer with six-bladed turbines in both the gas and liquid phases (Autoclave Engineers, Erie, PA) and was constructed with a heating/cooling mantle. A high-presssure membrane pump (Model DMK 30, Orlita AG, Geissen, Germany) with a maximum rating of 32.5 MPa and a 3-L/h flow rate was used to circulate the *n*-hexane solutions from the autoclave to the high-pressure IR cell and back to the autoclave via jacketed 1/8-in. (SS316) high-pressure tubing (Autoclave Engineers). The entire system, autoclave, transfer lines, and infrared cell, was cooled with a Polyscience cryostat (model 9505) and could be maintained isothermal ($\Delta T \leq 0.5$ °C) at 298−313 °C. Temperature measurements were made at the cryostat, autoclave, and IR cell with PT-100 thermoresistors. The necessary connections to vacuum and gases were made with 1/4-in (SS316) high-pressure tubing (Autoclave Engineers), and 1.0, 5.0, and 10.0 piezocrystals were used for pressure measurements (Keller AG, Winter, Switzerland). The

(14) Pino, P. J. *Organomet. Chem.* **1980**, *200*, 223.
(15) Lazzaroni, R.; Raffaelli, A.; Settambolo, R.; Bertozzi, S.; Vitulli, G. *J. Mol. Catal.* **1989**, *50*, 1.
(16) Van Rooy, A.; Oriji, E. N.; Kamer, P. C. J.; van Leeuwen, P. W. N. M. *Organometallics* **1995**, *14*, 34.
(17) Shriver, D. F.; Drezdzon, M. A. *The Manipulation of Air-Sensitive Compounds*; Wiley: New York, 1986.

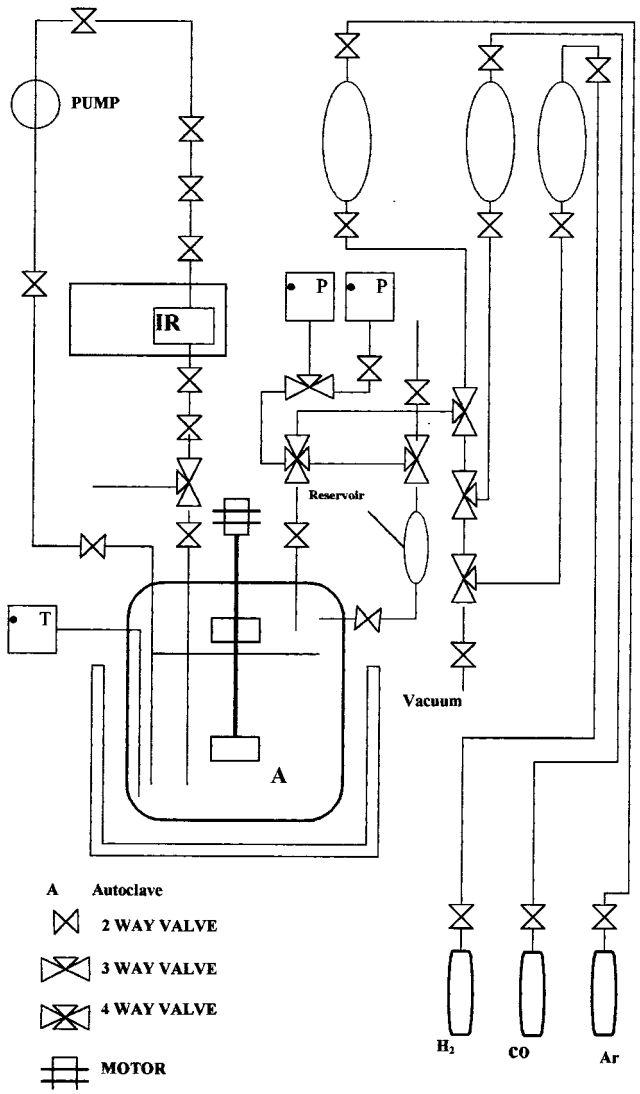


**Figure 1.** Schematic diagram of the appartus for high-pressure in-situ infrared spectroscopic and kinetic studies.

entire system was gastight under vacuum as well as at 20.0 MPa, the maximum operating pressure.

The high-pressure infrared cell was constructed at the ETH-Zürich of SS316 steel and could be heated and cooled. The $CaF_2$ single-crystal windows (Korth Monokristalle, Kiel, Germany) were 40-mm diameter by 15-mm thickness. Two sets of Viton and silicone gaskets provided sealing, and Teflon spacers were used between the windows. The construction of the flow through cell[18] is a variation on a design due to Noack[19] and differs in some respects from other high-pressure infrared cells described in the literature (for a review, see Whyman[20]). The high-pressure cell was situated in a Perkin-Elmer System 2000 Fourier transform infrared spectrometer. The resolution was set to 4 $cm^{-1}$ for all spectroscopic measurements. A schematic diagram of the experimental setup is shown in Figure 1.

**Spectroscopic Aspects.** Four normal infrared cells with $CaF_2$ windows were assembled for calibration. The optical path lengths were measured using the interference equations for parallel plates.[21] The measured optical pathlengths were 0.05. 0.215, 0.525, and 1.0 mm.

The infrared absorbance spectrum of the solvent *n*-hexane,[22] the reagent $C_8H_8$,[23] and the products (±)-$PhCH(CH_3)CHO$[24] and $PhCH_2CH_2CHO$[25] are all well documented. The solvent *n*-hexane has absorbance minima at 1120 and 1150 $cm^{-1}$ and an absorbance maximum at 1136 $cm^{-1}$. The absorptivity for *n*-hexane $\epsilon_{1136} = 1.969 \pm 0.045$ L/(mol cm) was determined with the four calibration cells and using the standard absorbance Lambert−Beer law where *c* is concentration in mol/L and *d* is the optical pathlength in cm.

$$A_i = \epsilon_i c_i d \tag{5}$$

The tetranuclear carbonyl $Rh_4(CO)_{12}$ has absorbance maxima at 2074, 2068, 2061, 2043, and 1885 $cm^{-1}$ in *n*-hexane.[26] The prominent band at 1885 $cm^{-1}$ is due to the stretching mode of the bridged carbonyl ligands. The absorptivity was determined in the high-pressure cell from absorbance data obtained at the beginning of four kinetic experiments, involving 50.5, 100.2, 150.8, and 198.7 mg $Rh_4(CO)_{12}$, after solvent subtraction. Each kinetic experiment initially involved 200 mL of *n*-hexane, 25 mL of styrene, and 5.0 MPa of CO. The experimentally determined absorptivity for $Rh_4(CO)_{12}$ in a solution of $C_8H_8$/*n*-hexane/CO was $\epsilon_{1885} = 6530 \pm 102$ L/(mol cm).

Calibrations for the two regioisomeric aldehydes were made using the integral absorbance law where *c* is concentration in mol/L and *d* is the optical pathlength in cm (eq 6). The major aldehyde (±)-$PhCH(CH_3)CHO$ has a prominent absorbance maximum at 1743 $cm^{-1}$ due to the C═O stretching mode.[27]

$$A^{I}_i = \epsilon^{I}_i c_i d \tag{6}$$

The integral absorptivity of (±)-$PhCH(CH_3)CHO$ was determined from five dilute solutions by dissolving 40, 130, 220, 310, and 400 $\mu$L in 40 mL of *n*-hexane and 5 mL of styrene. The experimentally determined integral absorptivity was $\epsilon^{I}_{1743} = 5430 \pm 98$ L/(mol cm). The minor aldehyde $PhCH_2CH_2CHO$ has a prominent absorbance maximum at 1735 $cm^{-1}$ due to the C═O stretching mode.[28] The absorptivity of $PhCH_2CH_2CHO$ was determined from five very dilute solutions by dissolving 10, 20, 30, 40, and 50 $\mu$L in 40 mL of *n*-hexane and 5 mL of styrene. The experimentally determined integral absorptivity was $\epsilon^{I}_{1735} = 4610 \pm 203$ L/(mol cm).

The major branched acyl intermediate (±)-$PhCH(CH_3)CORh(CO)_4$ has absorbance maxima at 2112, 2066, 2044, 2022, and 1692 $cm^{-1}$, and the minor unbranched acyl intermediate $PhCH_2CH_2CORh(CO)_4$ has absorbance maxima at 2112, 2066, 2044, 2022, and 1687 $cm^{-1}$. Spectra of each intermediate are shown in Figure 2. These were obtained by repeated subtractions from spectra obtained at different temperatures.

The assignment of the acyl intermediates was made by analyzing the series of four temperature-dependent kinetic experiments. By plotting the ratio of the branched/linear aldehyde concentrations versus the ratio of the integral absorbance of the bands 1692:1687, a linear proportionality

(18) Dietler, U. K. Ph.D. Dissertation 5428, ETH-Zurich, 1974.
(19) Noack, K. *Spectrochim Acta* **1968**, *24A*, 1917.
(20) Whyman, R. In *Laboratory Methods in Vibrational Spectroscopy*, 3rd ed.; Willis, H. A., van der Maas, J. H., Miller, R. G. J., Eds.; Wiley: New York, 1987; Chapter 12.
(21) Born, M.; Wolf, E. *Principles of Optics*; Pergamon: Oxford, 1975; p 360.
(22) (a) Pounchert, C. L. *The Aldrich Library of Infrared Spectra*; Aldrich: Milwaukee, WI, 1981; p 3. (b) *The Sprouse Collection of Infrared Spectra*; Hansen, D., Ed.; Sprouse Sc. Paoli: PA, 1990; Vol. 4, p 2.
(23) (a) Pounchert, C. L. *The Aldrich Library of Infrared Spectra*; Aldrich: Milwaukee, WI, 1981; p 30. (b) *The Sprouse Collection of Infrared Spectra*; Hansen, D., Ed.; Sprouse Sc. Paoli: PA, 1990; Vol. 4, p 40.
(24) Pounchert, C. L. *The Aldrich Library of Infrared Spectra*; Aldrich: Milwaukee, WI, 1981; p 280.
(25) Pounchert, C. L. *The Aldrich Library of Infrared Spectra*; Aldrich: Milwaukee, WI, 1981; p 280.
(26) (a) Beck, W.; Lottes, K. *Chem. Ber.* **1961**, *94*, 2378. (b) Bor, G.; Sbrignadello, G.; Noack, K. *Helv. Chim. Acta* **1975**, *58*, 815.
(27) Silverstein, R. M.; Bassler, G. C.; Morrill, T. C. *Spectroscopic Identification of Organic Compounds*, 4th ed.; Wiley: New York, 1981; p 119.
(28) Silverstein, R. M.; Bassler, G. C.; Morrill, T. C. *Spectroscopic Identification of Organic Compounds*, 4th ed.; Wiley: New York, 1981; p 119.

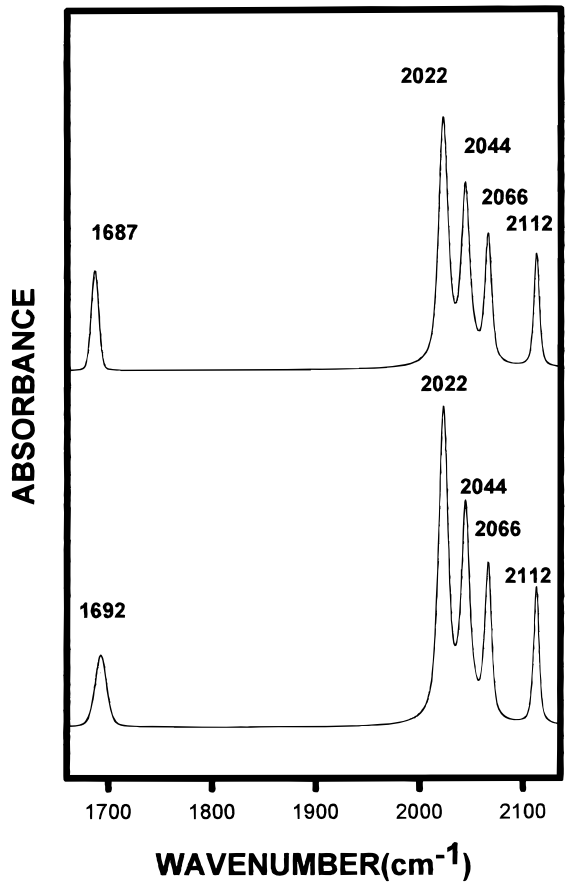


**Figure 2.** The in-situ pure component infrared spectra of the branched acyl rhodium tetracarbonyl (±)-$PhCH(CH_3)$-$CORh(CO)_4$ (below) and the linear acyl rhodium tetracarbonyl $PhCH_2CH_2CORh(CO)_4$ (above).

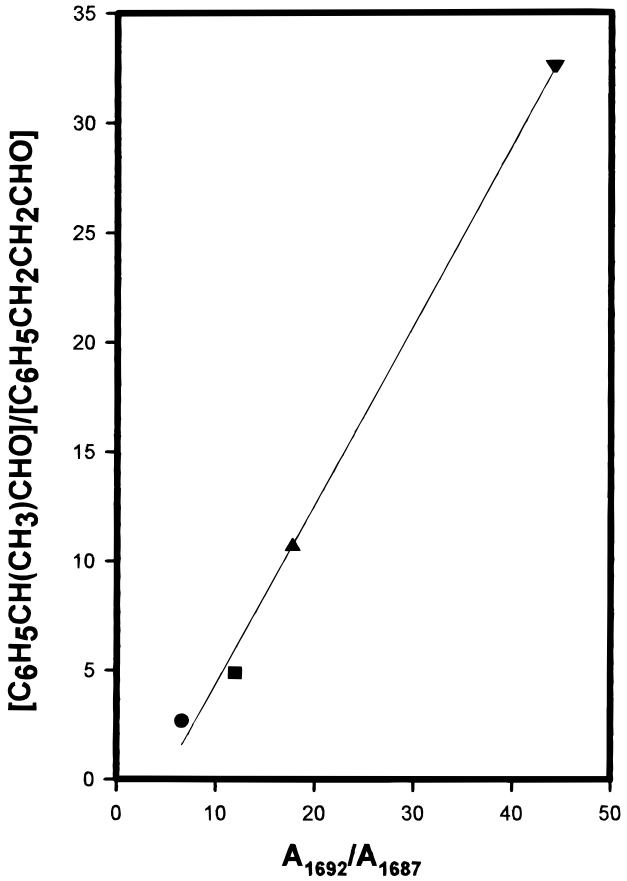


**Figure 3.** A plot of the ratio of branched-to-linear aldehyde versus integrated areas for branched and linear acyl rhodium tetracarbonyls.

was obtained.[29] Furthermore, it is clear from Figure 3 that the regioselectivities of the products observed in this study range from 2:1 to 32:1 in favor of the branched aldehyde. The regioselectivities reported are based on the in-situ spectroscopic measurement. However, they were confirmed, with a small margin of error, by GC.

The integral absorptivities of the major acyl intermediate (±)-$PhCH(CH_3)CORh(CO)_4$ at 1692 $cm^{-1}$ and minor acyl intermediate $PhCH_2CH_2CORh(CO)_4$ at 1687 $cm^{-1}$ were determined by employing a mole balance on rhodium and application of the dimensionless Lambert−Beer Law. The resulting expression is given in eq 7 where subscript $t_o$ denotes the beginning of each experiment and the subscript $t$ denotes any arbitrary time. Data from the 17 high-pressure kinetic experiments involving a total of 357 data points was used in the regression. The experimentally determined integral absorptivities, taken from the hydroformylation solutions consisting of $C_8H_8$/*n*-hexane/$CO/H_2$/aldehydes were $\epsilon^{I}_{1692} = 11400 \pm 324$ L/(mol $cm^{-1}$) and $\epsilon^{I}_{1687} = 9620 \pm 2280$ L/(mol $cm^{-1}$).

$$\left[\frac{4A_{Rh4}}{A_{hex}}\right]_{t_o} - \left[\frac{4A_{Rh4}}{A_{hex}}\right]_{t} = \left[\frac{A^{I}_{1687}}{A_{hex}}\right]_{t} \frac{\epsilon_{Rh4}}{\epsilon^{I}_{1687}} + \left[\frac{A^{I}_{1692}}{A_{hex}}\right]_{t} \frac{\epsilon_{Rh4}}{\epsilon^{I}_{1692}} \quad (7)$$

The mole fractions of the precursor $Rh_4(CO)_{12}$, the two acyl intermediates (±)-$PhCH(CH_3)CORh(CO)_4$ and $PhCH_2CH_2$-$CORh(CO)_4$ and the two aldehydes (±)-$PhCH(CH_3)CHO$ and $PhCH_2CH_2CHO$ were calculated during the hydroformylation experiments from in-situ absorbance measurements, using the dimensionless Lambert−Beer law (eq 8) in either its absorbance or integral absorbance form.[30] The term $x_{hex}$ is the known calculated mole fraction of *n*-hexane in the reaction mixture.

$$x_i = x_{hex}(A_i\epsilon_{1136})/(A_{1136}\epsilon_i) \quad (8)$$

The critical analytic bands chosen for quantitative measurements were the following: (±)-$PhCH(CH_3)CORh(CO)_4$ at 1692 $cm^{-1}$, $PhCH_2CH_2CORh(CO)_4$ at 1687 $cm^{-1}$, (±)-$PhCH(CH_3)$-CHO at 1742 $cm^{-1}$, and $PhCH_2CH_2CHO$ at 1735 $cm^{-1}$. In order to determine the absorbance due to each species, deconvolution and curve fitting was required in the region of 1660−1780 $cm^{-1}$. This was performed with the use of PeakFit. A typical result of the procedure is shown in Figure 4.

**Kinetic Studies.** Seventeen kinetic experiments in five sets were performed. These experiments differed due to the moles of $Rh_4(CO)_{12}$, the moles of styrene, the partial pressure of CO, the partial pressure of $H_2$, and the temperature.

Each experiment was executed in a similar manner. First, single-beam background spectra of the IR sample chamber were recorded, and then 150 mL of *n*-hexane was transferred under argon to the autoclave. Under 0.2 MPa of CO, infrared spectra of the *n*-hexane in the high-pressure cell were recorded. The total system pressure was raised to a predetermined MPa of CO, and the stirrer and high-pressure membrane pump were started. After equilibration, infrared spectra of the *n*-hexane/CO solution in the high-pressure cell were recorded. At this point, styrene was dissolved in 50 mL of *n*-hexane. This was transferred to a reservior, pressurized, and added to the

(29) Let rate(branched aldehyde) = $k_{br}(T)$[branched acyl complex] and let rate(linear aldehyde) = $k_{lin}(T)$[linear acyl complex]. The quotents are then {rate(branched)/rate(linear)} = $\{k_{br}(T)/k_{lin}(T)\}$-{[branched]/[linear]} where $\{k_{br}(T)/k_{lin}(T)\}$ must be positive.

(30) McClure, G. L. In *Laboratory Methods in Vibrational Spectroscopy*, 3rd ed.; Willis, H. A., van der Maas, J. H., Miller, R. G. J., Eds.; Wiley: New York, 1987; Chapter 7.

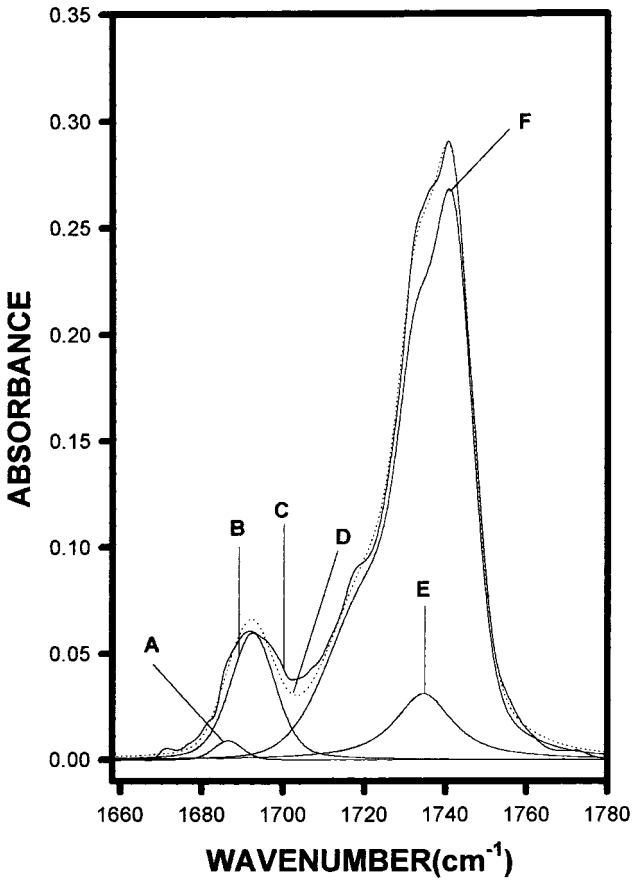


**Figure 4.** The integrated infrared areas for the two aldehyde functional groups and the two acyl functional groups in a typical in-situ experimental spectrum after deconvolution. A: $PhCH_2CH_2CORh(CO)_4$. B: (±)-$PhCH(CH_3)CORh(CO)_4$. C: total observable spectrum. D: Fitted spectrum. E: $PhCH_2CH_2CHO$. F: (±)-$PhCH(CH_3)CHO$.

autoclave. After equilibration, infrared spectra of the styrene/*n*-hexane/CO solution in the high-pressure cell were recorded. A solution of $Rh_4(CO)_{12}$ dissolved in 50 mL of *n*-hexane was prepared, transferred to the high-pressure reservior under argon, pressurized with CO, and then added to the autoclave. Infrared spectra of the $C_8H_8$/*n*-hexane/CO/$Rh_4(CO)_{12}$ solution in the high-pressure cell were recorded. The hydroformylation kinetic runs were then started by adding hydrogen. Spectra were recorded at 15 minute intervals over the interval of 1100−2200 $cm^{-1}$. A considerable number of spectral substractions were performed on each reaction spectrum in order to obtain the absorbance of $Rh_4(CO)_{12}$, the two acyl intermediates (±)-$PhCH(CH_3)CORh(CO)_4$ and $PhCH_2CH_2CORh(CO)_4$ and the two aldehydes (±)-$PhCH(CH_3)CHO$ and $PhCH_2CH_2CHO$ free of styrene, *n*-hexane, and CO absorbance.

The present hydroformylation reactions were performed under negligible gas−liquid mass transfer resistance. The experimentally measured overall mass transfer coefficients $K_La$ for hydrogen and carbon monoxide into *n*-hexane at 200 rpm was approximately 0.1 and 0.6 $s^{-1}$, respectively, as determined using the method of Deimling.[31] Since the maximium observed rate of hydroformylation in this study was $3 \times 10^{-6}$ mol $s^{-1}$, all experiments belong to the category of infinitely slow reaction with respect to gas−liquid mass transfer (i.e., the kinetic regime, Hatta category H).[32] The liquid phase of each experiment became essentially saturated with dissolved CO and $H_2$ in the first 60 s. Mass transfer effects are known to severely complicate the interpretation of kinetic data from hydroformylation reactions.[33]

In any single 5-h kinetic experiment, less than 0.054 mol conversion of $C_8H_8$ occurred (or maximum 17%). Therefore, the partial pressures of hydrogen and carbon monoxide in the closed-batch autoclave changed less than 2% during the each 5-h experiment. This partial pressure change was considered negligible, and hence, the liquid-phase concentrations of the two gaseous components were treated as constants for the duration of each experiment.

The rates of reaction, for the formation of the two aldehydes (±)-$PhCH(CH_3)CHO$ and $PhCH_2CH_2CHO$, were calculated from the concentrations using a central difference approximation. The central difference approximation was chosen since it provides an accurate approximation of derivative from sets of smooth monotonically increasing or decreasing experimental data.[34] In addition, extensive investigations concerning the numerical evaluation of turnover frequencies in homogeneous catalytic systems support the central difference approximation.[35]

**Solubilities.** Solubility data for hydrogen[36] and carbon monoxide[37] in *n*-hexane are available from the literature. The Henry constants were calculated using eqs 9 and 10, respectively, where the temperature $T$ is in Kelvin and $P_{sat}$ is the saturated vapor pressure of *n*-hexane.[38]

$$H_{H2}(P,T) = P_{sat}\exp(-4.96 + 4050/T)\exp(v_{H2}(P - P_o)/RT) \quad (9)$$

$$H_{CO}(P,T) = P_{sat}\exp(-5.05 + 3880/T)\exp(v_{CO}(P - P_o)/RT) \quad (10)$$

The derivation of the temperature-dependent form used can be found in the literature.[39] These equations are strictly valid only for pure hexane. The Krichevsky−Kasarnovsky correction for total pressure effects on the Henry constant has been included, where $P_o$ is the standard reference pressure 0.1 MPa.[40] The partial molar volumes of hydrogen and carbon monoxide in aliphatic hydrocarbons including *n*-hexane are $v_{H2}$ = 43 mL/mol[41] and $v_{CO}$ = 52 mL/mol.[42] Finally, both dissolved hydrogen and dissolved carbon monoxide were considered to be ideal solutes. No mixing rules were invoked in order to compensate for nonideality in the two-phase system, and the Krichevsky−Ilinskaya correction was not employed.[43]

## Kinetic Results

**Effects of Styrene.** The concentration of styrene was systematically varied in four hydroformylation experiments performed at 303 K with 5.0 MPa of carbon monoxide, 0.5 MPa of hydrogen, and 100 mg $Rh_4(CO)_{12}$

(31) Deimling, A.; Karandikar, B. M.; Shah, Y. T.; Carr, N. L. *Chem. Eng. J.* **1984**, *29*, 127.
(32) Levenspiel, O. *Chemical Reaction Engineering*; Wiley: New York, 1972; p 418.
(33) Bhattacharya, A.; Chaudari, R. V. *Ind. Eng. Chem. Res.* **1987**, *26*, 1168.
(34) Davies, M. E. *Numerical Methods and Modelling for Chemical Engineers*; Wiley: New York, 1984.
(35) Shirt, R.; Garland, M.; Rippin, D. W. T. *Anal. Chim. Acta* **1998**, *374*, 67.
(36) Nichols, W. B.; Reamer, H. H.; Sage, B. H. *AIChE J.* **1957**, *3*, 262.
(37) Koelliker, R.; Thies, H. *J. Chem. Eng. Data* **1993**, *38*, 437.
(38) Gallant, R. W. *Physical Properties of Hydrocarbons*; Gulf: Houston TX, 1968.
(39) Jonah, D. A. *Fluid Phase Equil.* **1983**, *15*, 173.
(40) (a) Krichevsky, I. R.; Kasarnovsky, T. S. *J. Am. Chem. Soc.* **1935**, *57*, 2168. (b) Dodge, B. F.; Newton, R. H. *Ind. Eng. Chem.* **1937**, *29*, 718.
(41) (a) Connolly, J. F.; Kandalic, G. A. *J. Chem. Thermodyn.* **1984**, *16*, 1129. (b) Walkley, J.; Jenkins, W. I. *Trans. Faraday Soc.* **1968**, *64*, 19.
(42) Handa, Y. P.; Benson, G. C. *Fluid Phase Equilib.* **1982**, *8*, 161.
(43) Krichevsky, I. R.; Ilinskaya, A. A. *Zh. Fiz. Khim. USSR* **1945**, *19*, 621.

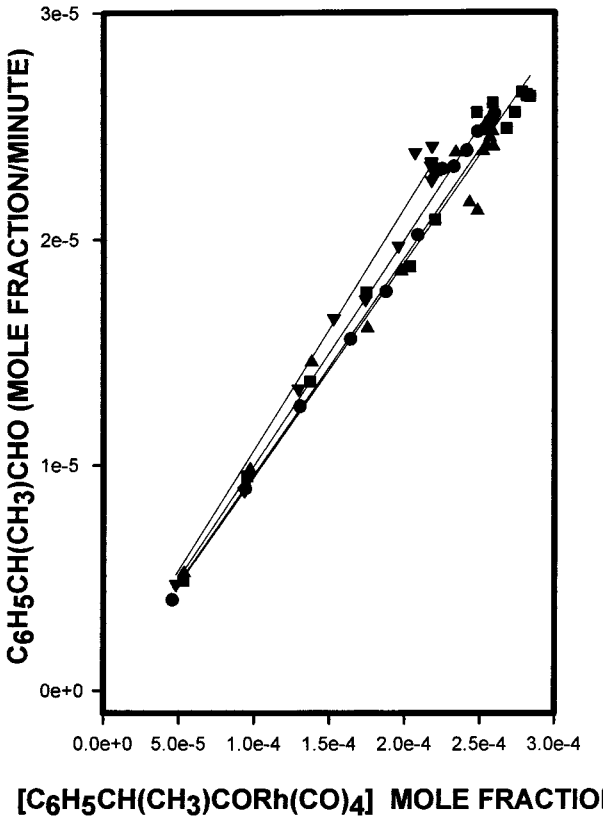


**Figure 5.** The rate of branched aldehyde versus the instantaneous branched acyl rhodium tetracarbonyl concentration. Styrene equals: ● 0.118, ■ 0.211, ▲ 0.286, ▼ 0.349 mol fraction.

by changing the amount of styrene used (20, 30, 40, 50 mL). The initial concentrations of styrene in mole fractions were $x_{styrene} = 0.118$, 0.211, 0.286, and 0.349 mol fraction. The corresponding initial concentrations of $Rh_4(CO)_{12}$, as measured by in-situ IR of the solution, were $7.20 \times 10^{-5}$, $6.12 \times 10^{-5}$, $4.70 \times 10^{-5}$, and $4.10 \times 10^{-5}$ mol fraction. About 6% conversion of styrene occurred in the four experiments.

As observed previously in our other kinetic study with 3,3-dimethylbut-1-ene as substrate,[9] the disappearance of the precursor $Rh_4(CO)_{12}$ during the initial phase of the hydroformylations with styrene is a well-behaved psuedo-first-order process over at least 2−3 half-lives. Equilibrium controlled precursor conversion, as observed with cyclohexene as substrate, did not occur.[11] The initial concentration of styrene did not have a strong effect on the rate. If the rate expression is taken to be $d[Rh_4(CO)_{12}]/dt = -k[Rh_4(CO)_{12}][C_8H_8]^{\alpha}$ where $k_{obs} = k[C_8H_8]^{\alpha}$, then the observable rate constants were $(1.75 \pm 0.02) \times 10^{-4}$, $(1.76 \pm 0.02) \times 10^{-4}$, $(2.07 \pm 0.06) \times 10^{-4}$, and $(1.99 \pm 0.09) \times 10^{-4}$ $s^{-1}$ for the four experiments with $x_{styrene} = 0.118$, 0.211, 0.286, and 0.349 mol fraction, respectively. The observed reaction order in sytrene was $\alpha_{styrene} = 0.15 \pm 0.07$.

A plot of the rate of formation of the branched (major) aldehyde (±)-$PhCH(CH_3)CHO$ versus the instantaneous concentration of the branched acyl intermediate (±)-$PhCH(CH_3)CORh(CO)_4$ is shown in Figure 5. As clearly shown by Figure 5, the rate of product formation is proportional to the instantaneous concentration of the organometallic intermediate. Furthermore, the concentration of styrene appears to have a minimal effect on the rates. If the rate expression is taken to be $d[PhCH(CH_3)CHO]/dt = k[PhCH(CH_3)CORh(CO)_4][C_8H_8]^{\beta}$ where $k_{obs} = k[C_8H_8]^{\beta}$, then the observable rate constants were $(1.63 \pm 0.02) \times 10^{-3}$, $(1.60 \pm 0.03) \times 10^{-3}$, $(1.58 \pm 0.05) \times 10^{-3}$, and $(1.83 \pm 0.04) \times 10^{-3}$ $s^{-1}$ for the four experiments with $x_{styrene} = 0.118$, 0.211, 0.286, and 0.349 mol fraction, respectively. The observed reaction order in sytrene was $\beta_{styrene} = 0.07 \pm 0.09$. The selectivity for the major branched aldehyde over the minor linear aldehyde was approximately 10:1.

Similarly, the rate of formation of the linear (minor) aldehyde $PhCH_2CH_2CHO$ was proportional to the instantaneous concentration of the linear acyl intermediate $PhCH_2CH_2CORh(CO)_4$, and styrene had a minimal effect on the rates. If the rate expression is taken to be $d[PhCH_2CH_2CHO]/dt = k[PhCH_2CH_2CORh(CO)_4][C_8H_8]^{\gamma}$ where $k_{obs} = k[C_8H_8]^{\gamma}$, then the observable rate constants were $(2.67 \pm 0.03) \times 10^{-3}$, $(2.17 \pm 0.04) \times 10^{-3}$, $(2.17 \pm 0.07) \times 10^{-3}$, and $(2.50 \pm 0.06) \times 10^{-3}$ $s^{-1}$ for the four experiments with $x_{styrene} = 0.118$, 0.211, 0.286, and 0.349 mol fraction, respectively. The observed reaction order in sytrene was $\gamma_{styrene} = -0.06 \pm 0.17$. It should also be noted that the $k_{obs}$ is the same as the turnover frequency (TOF), and therefore, the minor catalytic cycle which produces the linear product has a slightly higher TOF. The ratio of branched acyl to linear acyl complex was approximately 15:1.

**Effects of Hydrogen.** The concentration of hydrogen was systematically varied in four hydroformylation experiments performed at 303 K with 5.0 MPa of carbon monoxide, 100 mg of $Rh_4(CO)_{12}$, and 20 mL of styrene (0.118 mol fraction) by changing the partial pressure of hydrogen (0.27, 0.5, 0.76, 1.01 MPa). The concentrations of hydrogen in mole fractions were $x_{H2} = 0.0020$, 0.0037, 0.0056, and 0.0074 mol fraction. The corresponding initial concentrations of $Rh_4(CO)_{12}$, as measured by in-situ IR of the solution, were $7.10 \times 10^{-5}$, $7.20 \times 10^{-5}$, $7.00 \times 10^{-5}$, and $6.86 \times 10^{-5}$ mol fraction. A maximum of 7% conversion of styrene occurred in the four experiments.

The disappearance of the precursor $Rh_4(CO)_{12}$ was again a psuedo-first-order process. In addition, the concentration of hydrogen had a strong effect on the rate. If the rate expression is taken to be $d[Rh_4(CO)_{12}]/dt = -k[Rh_4(CO)_{12}][H_2]^{\alpha}$ where $k_{obs} = k[H_2]^{\alpha}$, then the observable rate constants were $(1.01 \pm 0.02) \times 10^{-4}$, $(1.62 \pm 0.07) \times 10^{-4}$, $(2.48 \pm 0.16) \times 10^{-4}$, and $(3.40 \pm 0.24) \times 10^{-4}$ $s^{-1}$ for the four experiments with $x_{H2} = 0.0020$, 0.0037, 0.0056, and 0.0074 mol fraction, respectively. The observed reaction order in hydrogen was $\alpha_{H2} = 0.93 \pm 0.05$.

A plot of the rate of formation of the branched (major) aldehyde (±)-$PhCH(CH_3)CHO$ versus the instantaneous concentration of the branched acyl intermediate (±)-$PhCH(CH_3)CORh(CO)_4$ is shown in Figure 6. As clearly shown by Figure 6, the rate of product formation is again proportional to the instantaneous concentration of the organometallic intermediate. Furthermore, the concentration of hydrogen appears to have a strong effect on the rates. If the rate expression is taken to be $d[PhCH(CH_3)CHO]/dt = k[PhCH(CH_3)CORh(CO)_4][H_2]^{\beta}$ where $k_{obs} = k[H_2]^{\beta}$, then the observable rate constants were $(1.03 \pm 0.04) \times 10^{-3}$, $(1.64 \pm 0.02) \times 10^{-3}$, $(2.35 \pm 0.08) \times 10^{-3}$, and $(3.34 \pm 0.10) \times 10^{-3}$ $s^{-1}$ for the four

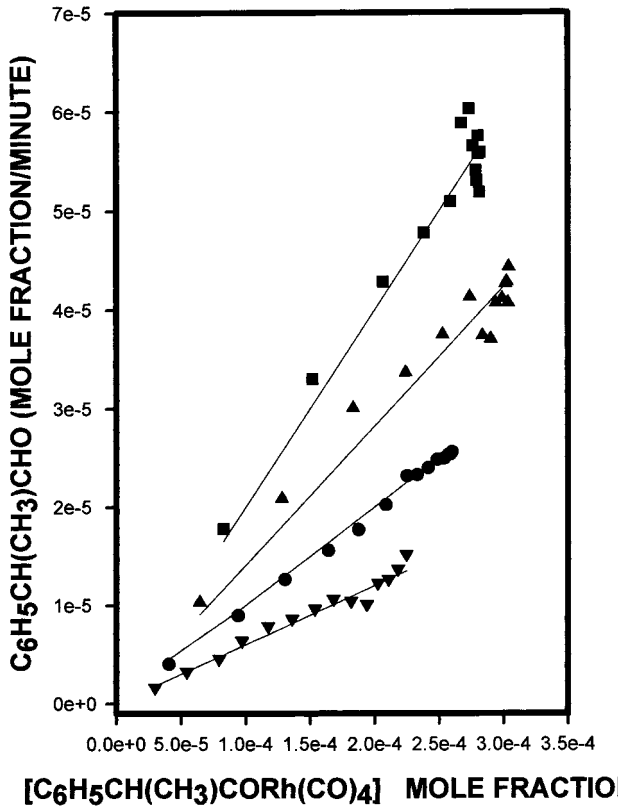


**Figure 6.** The rate of branched aldehyde versus the instantaneous branched acyl rhodium tetracarbonyl concentration. Hydrogen equals: ▼ 0.0020, ● 0.0037, ▲ 0.0056, ■ 0.0074 mol fraction.

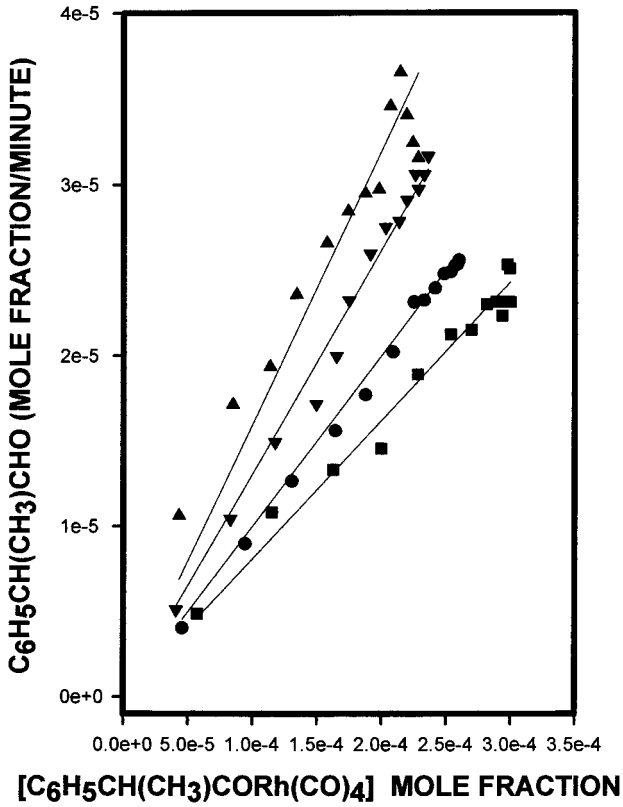


**Figure 7.** The rate of branched aldehyde versus the instantaneous branched acyl rhodium tetracarbonyl concentration. Carbon monoxide equals: ▲ 0.0414, ▼ 0.0534, ● 0.0635, ■ 0.0746 mol fraction.

experiments with $x_{H2}$ = 0.0020, 0.0037, 0.0056, and 0.0074 mol fraction, respectively. The observed reaction order in sytrene was $\beta_{H2} = 0.96 \pm 0.32$. The selectivity for the major branched aldehyde over the minor linear aldehyde was approximately 10:1.

Similarly, the rate of formation of the linear (minor) aldehyde $PhCH_2CH_2CHO$ was proportional to the instantaneous concentration of the linear acyl intermediate $PhCH_2CH_2CORh(CO)_4$, and hydrogen had a strong effect on the rates. If the rate expression is taken to be $d[PhCH_2CH_2CHO]/dt = k[PhCH_2CH_2CORh(CO)_4][H_2]^{\gamma}$ where $k_{obs} = k[H_2]^{\gamma}$, then the observable rate constants were $(1.68 \pm 0.07) \times 10^{-3}$, $(2.72 \pm 0.03) \times 10^{-3}$, $(3.23 \pm 0.11) \times 10^{-3}$, and $(5.78 \pm 0.18) \times 10^{-3}$ $s^{-1}$ for the four experiments with $x_{H2}$ = 0.0020, 0.0037, 0.0056, and 0.0074 mol fraction, respectively. The observed reaction order in hydrogen was $\gamma_{H2} = 0.94 \pm 0.34$. Since $k_{obs}$ is the same as the turnover frequency (TOF), the minor catalytic cycle which produces the linear product has the consistently higher TOFs. The ratios of branched acyl to linear acyl complex in the different runs was ca. 15:1.

**Effects of Carbon Monoxide.** The concentration of carbon monoxide was systematically varied in four hydroformylation experiments performed at 303 K with 0.5 MPa of hydrogen, 100 mg of $Rh_4(CO)_{12}$, and 20 mL of styrene (0.118 mol fraction) by changing the partial pressure of carbon monoxide (3.0, 4.0, 5.0, 6.0 MPa). The concentrations of carbon monoxide in mole fractions were $x_{CO}$ = 0.041, 0.053, 0.064, and 0.075 mol fraction. The corresponding initial concentrations of $Rh_4(CO)_{12}$, as measured by in-situ IR of the solution, were $7.04 \times 10^{-5}$, $7.20 \times 10^{-5}$, $7.20 \times 10^{-5}$, and $7.01 \times 10^{-5}$ mol fraction. A maximum of 7% conversion of styrene occurred in the four experiments.

The disappearance of the precursor $Rh_4(CO)_{12}$ was again a psuedo-first-order process. The concentration of carbon monoxide had a strong effect on the rate. If the rate expression is taken to be $d[Rh_4(CO)_{12}]/dt = -k[Rh_4(CO)_{12}][CO]^{\alpha}$ where $k_{obs} = k[CO]^{\alpha}$, then the observable rate constants were $(9.84 \pm 0.06) \times 10^{-5}$, $(1.36 \pm 0.04) \times 10^{-4}$, $(1.65 \pm 0.06) \times 10^{-4}$, and $(2.34 \pm 0.09) \times 10^{-4}$ $s^{-1}$ for the four experiments with $x_{CO}$ = 0.041, 0.053, 0.064, and 0.075 mol fraction, respectively. The observed reaction order in carbon monoxide was $\alpha_{CO} = 1.3 \pm 0.3$.

A plot of the rate of formation of the branched (major) aldehyde (±)-$PhCH(CH_3)CHO$ versus the instantaneous concentration of the branched acyl intermediate (±)-$PhCH(CH_3)CORh(CO)_4$ is shown in Figure 7. As clearly shown by Figure 7, the rate of product formation is again proportional to the instantaneous concentration of the organometallic intermediate. Furthermore, the concentration of carbon monoxide appears to have a strong effect on the rates. If the rate expression is taken to be $d[PhCH(CH_3)CHO]/dt = k[PhCH(CH_3)CORh(CO)_4][CO]^{\beta}$ where $k_{obs} = k[CO]^{\beta}$, then the observable rate constants were $(2.65 \pm 0.14) \times 10^{-3}$, $(2.18 \pm 0.05) \times 10^{-3}$, $(1.63 \pm 0.03) \times 10^{-3}$, and $(1.34 \pm 0.04) \times 10^{-3}$ $s^{-1}$ for the four experiments with $x_{CO}$ = 0.041, 0.053, 0.064, and 0.075 mol fraction, respectively. The observed reaction order in carbon monoxide was $\beta_{CO} = -1.0 \pm 0.7$. The selectivity for the major branched aldehyde over the minor linear aldehyde was approximately 10:1.

Similarly, the rate of formation of the linear (minor) aldehyde $PhCH_2CH_2CHO$ was proportional to the in-

stantaneous concentration of the linear acyl intermediate $PhCH_2CH_2CORh(CO)_4$, and the concentration of carbon monoxide had a strong effect on the rates. If the rate expression is taken to be $d[PhCH_2CH_2CHO]/dt = k[PhCH_2CH_2CORh(CO)_4][CO]^{\gamma}$ where $k_{obs} = k[CO]^{\gamma}$, then the observable rate constants were $(4.27 \pm 0.22) \times 10^{-3}$, $(3.47 \pm 0.08) \times 10^{-3}$, $(2.72 \pm 0.06) \times 10^{-3}$, and $(2.25 \pm 0.07) \times 10^{-3}$ $s^{-1}$ for the four experiments with $x_{CO} = 0.041$, 0.053, 0.064, and 0.075 mol fraction, respectively. The observed reaction order in hydrogen was $\gamma_{CO} = -0.9 \pm 0.6$. Since $k_{obs}$ is the same as the turnover frequency (TOF), the minor catalytic cycle which produces the linear product has the consistently higher TOFs. The ratios of branched acyl to linear acyl complex in the different runs was consistently circa 15:1.

**Effects of Temperature.** Temperature was systematically varied in four hydroformylation experiments performed with 0.5 MPa of hydrogen, 5.0 MPa of carbon monoxide, 100 mg of $Rh_4(CO)_{12}$, and 20 mL of styrene (0.118 mol fraction). The temperatures chosen were 298, 303, 308, and 313 K. The corresponding initial concentrations of $Rh_4(CO)_{12}$, as measured by in-situ IR of the solution, were $6.79 \times 10^{-5}$, $7.20 \times 10^{-5}$, $6.93 \times 10^{-5}$, and $7.27 \times 10^{-5}$ mol fraction. A maximum of 17% conversion of styrene occurred in the four experiments.

Again, the disappearance of the precursor $Rh_4(CO)_{12}$ was a psuedo-first-order process, and the temperature had a strong effect on the rate. If the rate expression is taken to be $d[Rh_4(CO)_{12}]/dt = -k_{obs}[Rh_4(CO)_{12}]$, then the observable rate constants were $(1.23 \pm 0.01) \times 10^{-4}$, $(1.64 \pm 0.02) \times 10^{-4}$, $(2.88 \pm 0.05) \times 10^{-4}$, and $(4.02 \pm 0.08) \times 10^{-4}$ $s^{-1}$ for the four experiments with $T = 298$, 303, 308, and 313 K, respectively. If $k_{obs}$ is expressed as $k_o[CO]^{1.3}[H_2]^{0.9}[C_8H_8]^{0.15}$, then the corresponding apparent activation parameters are $\Delta H^{\ddagger} = 62.6 \pm 5.3$ kJ/mol and $\Delta S^{\ddagger} = 37.3 \pm 17.4$ J/molK, where a small error is incurred due to temperature dependencies of the solubilities.

A plot of the rate of formation of the branched (major) aldehyde (±)-$PhCH(CH_3)CHO$ versus the instantaneous concentration of the branched acyl intermediate (±)-$PhCH(CH_3)CORh(CO)_4$ is shown in Figure 8. As clearly shown by Figure 8, the rate of product formation is again proportional to the instantaneous concentration of the organometallic intermediate. Furthermore, temperature appears to have a strong effect on the rates. If the rate expression is taken to be $d[PhCH(CH_3)CHO]/dt = k_{obs}[PhCH(CH_3)CORh(CO)_4]$, then the observable rate constants were $(0.93 \pm 0.03) \times 10^{-3}$, $(1.63 \pm 0.02) \times 10^{-3}$, $(3.13 \pm 0.10) \times 10^{-3}$, and $(4.18 \pm 0.07) \times 10^{-3}$ $s^{-1}$ for the four experiments with $T = 298$, 303, 308, and 313 K, respectively. If $k_{obs}$ is expressed as $k_o[CO]^{-1.0}[H_2]^{1.0}[C_8H_8]^{0.0}$, then the corresponding apparent activation parameters are $\Delta H^{\ddagger} = 78.8 \pm 17.3$ kJ/mol and $\Delta S^{\ddagger} = 15.2 \pm 56.6$ J/molK, where a small error is incurred due to temperature dependencies of the solubilities. The selectivities for the major branched aldehyde over the minor linear aldehyde ranged from a high of 32:1 at 298 K to a low of 2:1 at 313 K.

A plot of the rate of formation of the linear (minor) aldehyde $PhCH_2CH_2CHO$ versus the instantaneous concentration of the linear acyl intermediate $PhCH_2CH_2CORh(CO)_4$ is shown in Figure 9. As clearly shown by Figure 9, the rate of product formation is again proportional to the instantaneous concentration of the organometallic intermediate. Furthermore, temperature appears to have a strong effect on the rates. If the rate expression is taken to be $d[PhCH_2CH_2CHO]/dt = k_{obs}[PhCH_2CH_2CORh(CO)_4]$, then the observable rate constants were $(1.27 \pm 0.05) \times 10^{-3}$, $(2.72 \pm 0.03) \times 10^{-3}$, $(7.68 \pm 0.24) \times 10^{-3}$, and $(10.3 \pm 0.2) \times 10^{-3}$ $s^{-1}$ for the four experiments with $T = 298$, 303, 308, and 313 K, respectively. If $k_{obs}$ is expressed as $k_o[CO]^{-1.0}[H_2]^{1.0}[C_8H_8]^{0.0}$, then the corresponding apparent activation parameters are $\Delta H^{\ddagger} = 113 \pm 33$ kJ/mol and $\Delta S^{\ddagger} = -102 \pm 109$ J/molK, where a small error is incurred due to temperature dependencies of the solubilities. Since $k_{obs}$ is the same as the turnover frequency (TOF), the minor catalytic cycle which produces the linear product has the consistently higher TOFs at all temperatures. Also, comparison of Figures 8 and 9 shows that the ratios of branched acyl to linear acyl complex in the different runs change from a high of ca. 40 at 298 K to ca. 7 at 313 K. Figure 9 indicates that the amount of the linear acyl complex is particularly temperature dependent.

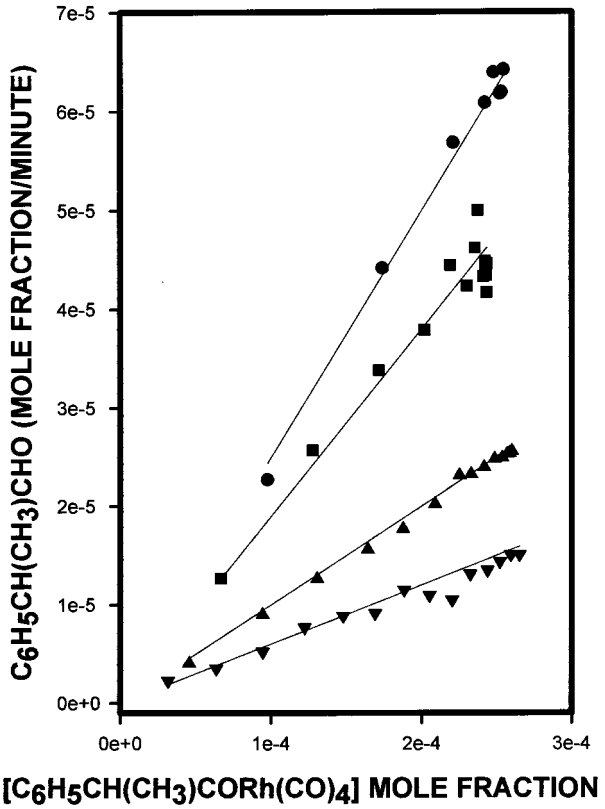


**Figure 8.** The rate of branched aldehyde versus the instantaneous branched acyl rhodium tetracarbonyl concentration. Temperature equals: ▼ 298 K, ▲ 303 K, ■ 308 K, ● 313 K.

## Discussion

The overall kinetics of the dual-cycle regioselective hydroformylation of styrene are conveniently separated into the kinetics associated with the cluster fragmentation of $Rh_4(CO)_{12}$, which essentially defines the induction period, and those kinetics associated with the hydrogenolysis of the two acyl intermediates. The latter

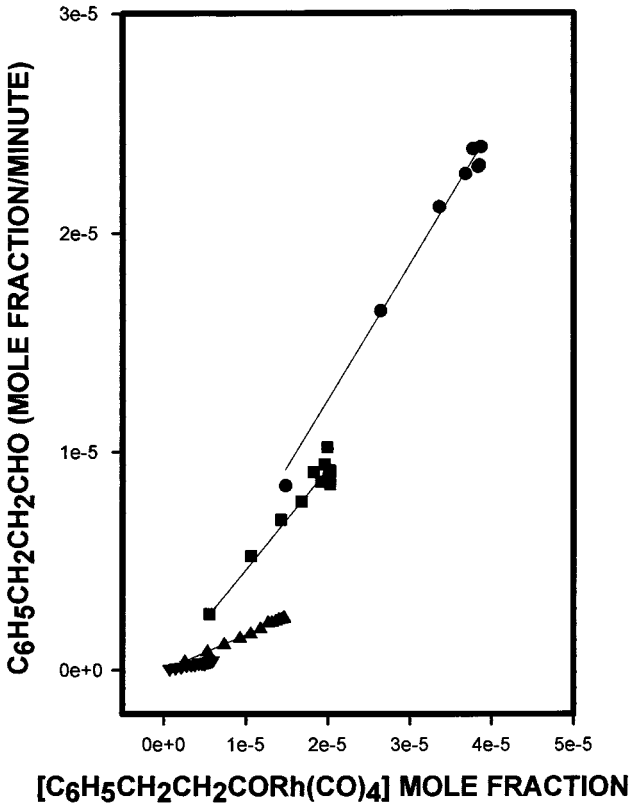


**Figure 9.** The rate of linear aldehyde versus the instantaneous linear acyl rhodium tetracarbonyl concentration. Temperature equals: ▼ 298 K, ▲ 303 K, ■ 308 K, ● 313 K.

kinetics are readily transformed into the classic representation for turnover frequencies.

**The Induction Period and Cluster Fragmentation.** Under the hydroformylation reaction conditions, the tetranuclear precursor $Rh_4(CO)_{12}$ underwent cluster fragmentation. The eventual outcome of this fragmentation was the formation of the two observable mononuclear acyl rhodium intermediates. Thus the fragmentation kinetics represent, to a good approximation, the induction period for the catalytic system. The salient form of the fragmentation kinetics took the functional form:

$$\frac{d[Rh_4(CO)_{12}]}{dt} = k^{\alpha}_{o}[Rh_4(CO)_{12}]^{1.0}[CO]^{1.3}[H_2]^{1.0}[C_8H_8]^{0.15} \quad (11)$$

$$k^{\alpha}_{o} = \frac{\kappa T}{h}\exp\left[\frac{-62.6\ \text{kJ}}{\text{mol}\ RT} + \frac{37.3\ \text{J}}{\text{mol K}\ R}\right] \quad (12)$$

In previous detailed kinetic studies of unicylic hydroformylation systems using $Rh_4(CO)_{12}$ as catalyst precursor, a very similar functional form has been found. Indeed, in the hydroformylation of 3,3-dimethylbut-1-ene, the fragmentation kinetics took the form $[Rh_4(CO)_{12}][CO]^{1.7}[H_2]^{0.7}[33DMB]^{0.1}$.[9] This strongly suggests that the same mechanism is operative, and perhaps generally applicable to $Rh_4(CO)_{12}$ hydroformylations. The high overall reaction order is most readily rationalized in terms of CO-assisted polyhedron opening (or perhaps, equilibrated polyhedron opening) followed by oxidative addition of hydrogen as the rate-limiting step. Indeed, numerous cases of CO assisted cluster polyhedron opening are documented.[44] The low order in alkene only serves to indicate that alkene must be present to react with the resulting hydrido rhodium complexes.

With regard to the activation parameters, the enthalpy of activation indicates the dissociation of one or more Rh−Rh bonds, whereas the low entropy of activation indicates that the polyhedron opening is compensated by the addition of new ligands. In our previous study,[9] the experimentally activation parameters for this cluster fragmentation were $\Delta H^{\ddagger} = 74.4 \pm 12.0$ kJ/mol and $\Delta S^{\ddagger} = 17.8 \pm 2.9$ J/(mol K).

**The Regioselectivity and the Turnover Frequencies.** The hydrogenolysis of the the two acyl rhodium intermediates represents the rate-limiting step for aldehyde formation for each of the two catalytic cycles of the dual-cycle catalytic mechanism. In the case of the hydrogenolysis of the major branched acyl intermediate (±)-$PhCH(CH_3)CORh(CO)_4$ to form the major branched aldehyde (±)-$PhCH(CH_3)CHO$, the rate of hydrogenolysis took the form:

$$\frac{d[PhCH(CH_3)CHO]}{dt} = k^{\beta}_{o}[PhCH(CH_3)CORh(CO)_4]^{1.0}[CO]^{-1.0}[H_2]^{1.0}[C_8H_8]^{0.0} \quad (13)$$

$$k^{\beta}_{o} = \frac{\kappa T}{h}\exp\left[\frac{-78.6\ \text{kJ}}{\text{mol}\ RT} + \frac{15.2\ \text{J}}{\text{mol K}\ R}\right] \quad (14)$$

In the case of the hydrogenolysis of the minor linear acyl intermediate $PhCH_2CH_2CORh(CO)_4$ to form the minor linear aldehyde $PhCH_2CH_2CHO$, the rate of hydrogenolysis took the form:

$$\frac{d[PhCH_2CH_2CHO]}{dt} = k^{\gamma}_{o}[PhCH_2CH_2CORh(CO)_4]^{1.0}[CO]^{-1.0}[H_2]^{1.0}[C_8H_8]^{0.0} \quad (15)$$

$$k^{\gamma}_{o} = \frac{\kappa T}{h}\exp\left[\frac{-112.8\ \text{kJ}}{\text{mol}\ RT} + \frac{-102\ \text{J}}{\text{mol K}\ R}\right] \quad (16)$$

The functional forms of the hydrogenolysis unambiguously support the conclusion that equilibrated carbonyl dissociation is the first step and irreversible hydrogen activation is the second. In the cases of the hydroformylation of 3,3-dimethylbut-1-ene starting with $CoRh(CO)_7$ as precursor,[45] the hydroformylation of 3,3-dimethylbut-1-ene starting with $Rh_4(CO)_{12}$ as precursor,[9] and the hydroformylation of cyclohexene starting with $Rh_4(CO)_{12}$ as precursor,[11] the corresponding acyl rhodium tetracarbonyls were formed, and the experimentally determined form of the hydrogenolysis was always the same, namely $[RCORh(CO)_4]^{1.0}[CO]^{-1.0}[H_2]^{1.0}[alkene]^{0.0}$. Furthermore, the measured enthalpies of activation were 49.3 and 84.6 kJ/mol and the entropies of activation were −8.7 and 121 J/(mol K) for 3,3-dimethylbut-1-ene and cyclohexene, respectively.

(44) (a) Bor, G.; Dietler, U. K.; Pino, P.; Poe, A. *J. Organomet. Chem.* **1978**, *154*, 301. (b) Knoll, K.; Huttner, G.; Zsolnai, L.; Jibril, I.; Wasiucionek, M. *J. Organomet. Chem.* **1985**, *294*, 91. (c) Geoffroy, G. L.; Foley, H. C.; Fox, J. R.; Gladfelter, W. L. *ACS Symp. Ser.* **1981**, *155*, 111.

(45) Garland, M. Ph.D. Dissertation 8585, ETH-Zurich, 1988.

Since the acyl rhodium tetracarbonyls are the only observable intermediates during the hydroformylation, their concentrations serve as a very good approximation to the total concentration of intermediates in each cycle. Accordingly, the turnover frquencies for branched and linear aldehyde formation are

$$\mathrm{TOF(branched)} = k^{\beta}_{o}[\mathrm{CO}]^{-1.0}[\mathrm{H_2}]^{1.0} \qquad (17)$$

$$\mathrm{TOF(linear)} = k^{\gamma}_{o}[\mathrm{CO}]^{-1.0}[\mathrm{H_2}]^{1.0} \qquad (18)$$

In this context, it should be repeated that the branched aldehyde cycle exhibited the slowest TOF and consequently highest accumulated concentrations of acyl intermediate, whereas, the linear aldehyde cycle had the highest TOF and hence the lowest accumulated concentration of acyl intermediate.

The selectivity for the branched aldehyde (br-ald) is now readily written in terms of the concentrations of the acyl intermediates and the turnover frequencies as

$$s^{\mathrm{br-ald}} = \frac{[\text{br-acyl}]\mathrm{TOF(branched)}}{[\text{br-acyl}]\mathrm{TOF(branched)} + [\text{lin-acyl}]\mathrm{TOF(linear)}} \qquad (19)$$

where br-acyl is branched acyl and lin-acyl is linear acyl.

As previously mentioned, the selectivities to the two acyl rhodium intermediates are, to a good approximation, only temperature dependent. If $s^{\mathrm{br-acyl}}(T)$ and $s^{\mathrm{lin-acyl}}(T)$ are used to designate the temperature-dependent selectivities for the formation of acyl rhodium intermediates, and their sum must equal unity, then eq 19 is easily rewritten in terms of the selectivities of the intermediates and turnover frequencies alone.

## Conclusions

In-situ spectroscopic and kinetic measurements of the regioselective unmodified rhodium-catalyzed hydroformylation of styrene to (±)-2-phenylpropanal and 3-phenylpropanal were performed. A wide range of reaction conditions were studied. In all experiments, the decomposition of the precursor $Rh_4(CO)_{12}$ was observed under reaction conditions, resulting in the formation of two observable acyl intermediates, namely, the major isomer (±)-$PhCH(CH_3)CORh(CO)_4$ and the minor isomer $PhCH_2CH_2CORh(CO)_4$. Concurrent formation of the corresponding branched and linear aldehydes was also observed.

The observable kinetics of the entire system, namely, the induction kinetics and the product formation kinetics, were examined. The functional form for the cluster fragmentation of the precursor to give rise to the acyl rhodium tetracarbonyl intermediates was experimentally determined. The functional form strongly suggests CO assisted polyhedron opening as the first step.

With regard to product formation, the inherent 3-cycle catalytic mechanism, resulting in (−)-2-phenylpropanal, (+)-2-phenylpropanal, and 3-phenylpropanal, was analyzed from the viewpoint of a condensed 2-cycle or dual-cycle mechanism. Since only one rhodium intermediate on each of the two cycles was observable, e.g., (±)-$PhCH(CH_3)CORh(CO)_4$ and $PhCH_2CH_2CORh(CO)_4$, the decomposition of the product formation kinetics was easily accomplished in terms of the respective turnover frequencies. The functional forms of the hydrogenolysis kinetics unambiguously suggest a mechanism consisting of the loss of a CO ligand followed by hydrogen activation.

Consistent with numerous previously reported experimental studies, the unmodified rhodium-catalyzed hydroformylation of styrene results in the preferential formation of the branched aldehyde. In this study, it was observed that the branched acyl rhodium tetracarbonyl was also the predominant acyl complex in solution. However, the efficiency of the linear aldehyde producing cycle in the dual-cycle mechanism is higher as verified by its larger turnover frequency.

OM980514V